Update on Geological constraints on biohabitats: A geophysical characterization of San Diego Bay and adjacent regions

by

Scripps Institution of Oceanography, University of California, San Diego, La Jolla, California 92093

San Diego State University, San Diego, California

Executive Summary

Swath bathymetry and high-resolution CHIRP data were acquired in San Diego Bay to examine the relationship between geologic substrate exposed at or near the seafloor and related biohabitats. The data reveal important links between geology and biohabitats. For example, south of Ballast Point where the transgressive surface outcrops and exposes hard grounds on the seafloor exist kelp beds not observed in other regions within the bay. Likewise, at the bay mouth the Point Loma Formation outcrops on the seafloor as a horst block that provides a hold fast for other varieties of kelp. In addition, the overall density of seagrass exhibits depth control along Zuniga Jetty; the density of seagrass decreases with depth. Nevertheless, secondary controls on seagrass density are observed and appear to be related to rapid sedimentation associated with sediment spillways in the Zuniga Jetty. Terrestrial sediment input into the bay is low. Regions of modern sediment accumulation near the Embarcadero and south of Ballast Point appear to be caused by anthropogenic sediment reworking related to ship traffic. Recency of offset along existing faults (Spanish Bight, Coronado, and Silver Strand faults) as well as a newly identified fault, was examined using the CHIRP data. These faults have a dip-slip transtensional component and appear to be active in the Holocene, with some exhibiting a

bathymetric expression. As such these faults, in all likelihood, play a role in groundwater flux and stream capture of the San Diego River in the past. In summary, these geophysical investigations of San Diego Bay and surrounding regions have yielded new insights into the operative processes that shape the bay as well as providing a quantitative baseline from which future change can be assessed (e.g., rapid sea level rise $\geq$ 3 mm/yr).

INTRODUCTION

The near shore region of San Diego is facing increased pressures from fisheries, land development and runoff, as well as climate change. Sea level is rising at an unprecedented rate of over 3 mm/yr due to global warming (IPCC, 2007; Rahmstorf, 2007; Pfeffer et al., 2008), raising concerns about the long-term stability of biogenic habitats in bays and estuaries. Our understanding of biological and geological processes in near shore regions remains limited; thus the response of near shore habitats (e.g., beaches, bays, and the inner shelf) to rapid sea level rise is difficult to predict. Understanding the factors that influence and limit the distribution, density, and patchiness of biogenic habitats in and around San Diego Bay is the critical first step toward developing predicative capabilities. Toward this goal, we have surveyed San Diego Bay and adjacent regions with swath bathymetry and subbottom CHIRP data to establish a regional baseline to evaluate change in response to a number of forcing factors (Fig. 1).

In San Diego Bay, anthropogenic influence is evident and, as such, the bay provides a laboratory to study how human constructs and natural processes interact to influence circulation, morphology, sediment processes, and ecosystem structure in near shore environments. San Diego bay is a tectonically active pull-apart basin that has undergone major deformation (Rockwell, 2010; Maloney et al., in prep.). Drainage to the bay has been altered through damming of rivers and altered drainage patterns, artificial islands have been constructed, and extensive dredging has removed sediment to maintain open shipping channels (Canada, 2006). Despite all of this overprinting, there are still large areas that are important for understanding the natural links between biology and geology where previous geologic structures and ongoing sediment transport play a role in

habitat distribution. Furthermore, the bay provides insights into the tectonic evolution of pull-apart basins (Basile and Brun, 1998; Katzman et al., 1995; McClay and Dooley, 1995; Wu et al., 2009) and how segmentation and stepovers along fault systems can influence the exposed geologic strata on the seafloor and associated biohabitats

We conducted geophysical surveys of the bay and surrounding region to understand the links between geology and biology and how anthropogenic impacts can alter or overprint these regions in the bay. We also imaged extensive faulting throughout the bay at high resolution to assess potential geohazards posed to the region. With ongoing and predicted future sea level rise (IPCC, 2007; Rahmstorf, 2007; Pfeffer et al., 2008), it is critical to understand the geologic controls on coastal morphology and how these forcing factors impact ecosystem structures.

BACKGROUND

San Diego Bay is ~25 km long and varies in width between 1-3 km (Fig. 2A). The bay is elongated along a trend of ~N10°W, but in the northwest, makes an almost 180° turn such that the mouth opens to the south. The depth of the bay ranges from ~15 m in the dredged shipping channel to < 1 m in the south. The ~100 m high Point Loma peninsula on the western edge of the bay mouth protects the bay from west and northwest waves and storms (Fig. 2B). Likewise, the Zuniga Jetty, which extends south from Coronado Island, protects the mouth of the bay along the eastern edge. Coronado Island was originally divided by a shallow channel (the Spanish Bight) into two land masses, North Island and Coronado Island. The bight was infilled and a naval base currently occupies what was once North Island, while old Coronado Island is primarily residential. The Silver Strand is a natural barrier beach connecting Imperial Beach to Coronado

Island, formed by sediment transport northward from the Tijuana River mouth (Elliott, 1987). Archeological evidence suggests that the Silver Strand formed ~5 ka when the rate of eustatic sea level rise decreased (Masters, 2006).

There are three main drainage channels into San Diego Bay from the east. These are Chollas Creek, Sweetwater River, and Otay River, and together they drain ~700 km^2 of combined urban, agricultural, and undeveloped land (Mazor and Schiff, 2007a; 2007b; 2007c). The Sweetwater and Otay rivers are dammed. The bay is considered a Mediterranean, inverse estuary, characterized by freshwater input almost exclusively during the winter with evaporation outpacing input for most of the year (Delgadillo-Hinojosa et al., 2008). This results in hypersalinity and long residence times for water in the bay (Largier et al., 1997). Average rainfall for San Diego is ~25 cm/yr (Largier, 1995). San Diego Bay shows seasonal variability and longitudinal gradients from the mouth to head of the bay in temperature, salinity, and nutrients (Delgadillo-Hinojosa et al., 2008). Over a year long study, with data collection in August, January, May and September, Delgadillo-Hinojosa et al. (2008) measured an overall temperature range of 13.5° C - 24.9° C and a salinity range of 32.27 - 35.86. Seasonal variability in salinity occurs mainly near the head of the bay, with measurements near the mouth remaining constant throughout the year. Estimates of overall residence times for San Diego Bay range from 2 - 100 days (Chadwick and Largier, 1999).

Circulation is driven by tidal pumping and the amount of exchange between the bay and the Pacific Ocean varies with tidal range (Chadwick and Largier, 1999). Currents are strongest at the mouth of the bay (50-100 cm/s) where the tidal influence is greatest, and weakest in the southern bay (<10 cm/s) (Chadwick and Largier, 1999). Modeled

transport of suspended fine-grained sediment (2 and 20 micron) out of San Diego Bay is ~4.7 x 10^7 kg/yr and input from rivers is ~2.25 x 10^7 kg/yr (Peng and Zeng, 2007).

Humans have been modifying San Diego Bay for over two centuries. In the early 1800s the San Diego River changed course from emptying into Mission Bay to emptying into San Diego Bay (Pourade, 1960). By the early 1850s there was significant concern that sediment input from the San Diego River would endanger use of the bay as a harbor. By 1877, a levee was built diverting flow of the river to Mission Bay permanently (Rambo and Speidel, 1969). In the 1900s San Diego Bay underwent extensive dredging and development projects resulting in loss of ~90% of natural marshland and ~50% of natural intertidal land. Harbor and Shelter Islands are both artificially constructed (Fig. 2A). The land surrounding the bay is developed into commercial, industrial, and military operations. Dredging of the main shipping channel and several marinas is ongoing, with the most recent major dredging effort conducted in 2004. Current protected areas include parts of the Point Loma peninsula, which is home to the Cabrillo National Monument, and the San Diego Bay National Wildlife Refuge, which encompasses ~2,600 acres of land and water in southern San Diego Bay (Service, 2006).

Regional Tectonics

Coastal San Diego is located at the boundary between the offshore inner California borderlands geologic province and the onshore Penninsular Ranges province. The region is characterized by several stike slip fault systems that accommodate motion between the Pacific and North American plates, and control San Diego geomorphology (Fig. 2A; Kennedy and Welday, 1980). San Diego Bay is a pull-apart basin formed by a

right step from offshore faults to the onshore Rose Canyon fault. The offshore faults involved in the step-over include the Coronado Bank fault and the Descanso fault.

The Descanso and Coronado Bank fault zones parallel one another trending northwest offshore San Diego (Fig. 1). The Descanso fault was mapped between the US-Mexico border and Point Loma (Legg, 1985) and appears associated with a basement horst-graben structure formed by localized dip-slip on the Coronado Bank fault (Maloney et al., in prep). The Coronado Bank fault may be a southern extension of the Palos Verdes fault zone, but recent surficial evidence suggests this may not be a through-going fault (Ryan et al., 2012); however, the faults may connect at depth in the basement. Another option is that only the northern and southern segments have ruptured recently with the intervening section being more quiescent (Fig. 1). Deformation in the offshore ICB is accommodated by predominantly strike-slip with localized areas of compression and extension at fault bends and steps. Offshore San Diego Bay, the Coronado bank fault exhibits localized extension that appears associated with the pull-apart basin (Maloney et al. in prep).

The Rose Canyon fault is the southern extension of the Newport Inglewood fault zone, which is located along the eastern side of Palos Verdes in Los Angeles County and steps offshore and trends along the shelf edge through Orange and San Diego Counties. At Point La Jolla, the Rose Canyon fault steps back onshore at a restraining bend responsible for the Mount Soledad topographic high (Rockwell, 2010). South of Mount Soledad, the fault zone trends ~N20°W and appears to terminate near downtown San Diego. Here, several faults splay into San Diego Bay and accommodate subsidence

across the basin. The slip rate on the Rose Canyon fault is ~1.5 mm/yr, with evidence for at least three events during the last ~8 kyr (Lindvall and Rockwell, 1995).

The San Diego Bay basin is ~20 km wide and ~2-3 km deep, and is filled with ~1-3 km thick sedimentary fill with increasing thickness to the south (Marshall, 1989). Fault trends and dips suggest an asymmetric pull-apart with ~10 km separation between the offshore Descanso fault and onshore Rose-Canyon fault. Three north-south trending fault zones extend south from near downtown, cross Coronado Island, and extend offshore. These are the Spanish Bight fault, Coronado fault, and Silver Strand fault. Several un-named faults have also been mapped in the southeastern bay (Fig. 2B). Several faults within the Bay extend to within 2-3 m of the bay floor and are likely Holocene active based on seismic reflection data and radiocarbon dating (Kennedy and Clarke, 1999). To the east, the north-south trending La Nacion fault zone has been interpreted as the eastern boundary of the pull-apart basin. The fault zone is composed of west-dipping, anastomosing normal faults with >60 m vertical offset observed in the Pliocene San Diego Formation (Hart, 1974).

Historic seismicity has been observed in the San Diego Bay vicinity. Astiz and Shearer (2000) located several earthquakes occurring between 1981 and 1997 of M<4 between Coronado Bank and Point Loma, which could be attributed to motion along either the Coronado Bank fault or the Descanso fault. Additional seismicity includes a pair of M3-4 earthquakes offshore Point Loma in 2006 (Caltech database ***), a M5.3 earthquake along the Coronado Bank fault in 1984 and reports of a large ~M6.0 earthquake offshore in 1862. Small magnitude earthquake clusters were also recorded near San Diego in 1964 (Simons, 1979) and 1985 (Reichle et al., 1985; Magistrale, 1993).

Ecosystems

Seagrass beds are an important component of shallow coastal waters, bays and estuaries. They provide food, refuge, and habitat space for many organisms, including commercially relevant fish and shellfish, and are important for nutrient cycling and sediment stabilization (Hemminga and Duarte, 2000). Several studies have documented loss or decline of seagrass ecosystems worldwide due to human impacts, which include increased sediment and nutrient supply, and fragmentation due to coastal development (e.g. Duarte, 2002; Orth et al., 2006; Short and Wyllie-Echeverria, 1996; Waycott et al., 2009). Efforts at restoring seagrass habitat often include artificial transplantation, although the success of this method is estimated at only ~30% (Fonseca et al., 1998). Light availability is the major requirement for seagrass habitat, as they require some of the highest levels of any plant group worldwide (Dennison et al., 1993, from Orth, 2006). As such, factors affecting the availability of light are most often studied, while other factors that may influence habitat, such as sediment characteristics, are less well understood (Koch, 2001). Nonetheless, erosional events (Bell 1999, Hine 1987 from Koch), variable sedimentation rates (Marba and Duarte, 1995 and Moore, 1993 from Koch), and bedform structure (Daniell et al., 2009) have been shown to impact seagrass populations.

METHODS

Between 2006 and 2012, over 1000 km of seismic chirp (compressed high intensity radar) data were acquired in and offshore San Diego Bay (Fig. 2). The data were collected using SIO's Edgetech Chirp profiler. The Chirp profiler was operated with a 50 ms swept pulse of 1-15 kHz, and provided sub-meter vertical resolution with sub-bottom penetration up to ~50 m. Location accuracy is to within 5 m. Chirp data were processed using sioseis (sioseis.ucsd.edu) (Henkart, 2003) and imported to Kingdom Suite (http://www.ihs.com) and QPS Fledermaus (http://www.qps.nl/display/fledermaus/main) software packages for interpretation. A nominal water and sediment velocity of 1500 m/s was assumed for all depth conversions in Chirp data.

Bathymetric data were acquired in 2012 using a Reson 7125 multibeam system operated at 400 kHz (Fig. 2) with a nominal vertical resolution of ~2.5 cm. Positions were calculated through a real time kinematic GPS system, providing centimeter lateral position accuracy. Data positions were determined using the Geoid99 model and are referenced to the NAVD88 vertical datum. Data were processed using Caris HIPS and SIPS software, and interpreted with IVS Fledermaus and ArcGIS software packages. In order to visualize the distribution of seagrass and kelp plants, these signals were not removed from the bathymetric data to make a bare Earth model.

RESULTS

Sediment

We observe several anthropogenic sedimentary features in the bay including dredge scours, cable trenches, pipelines, and shoals. Most scour features are observed within the dredged channel (e.g., Fig. 3A). A prominent set of linear, cross-channel trenches is observed trending north-northeast north of the Coronado Bridge between downtown San Diego and Coronado Island (Fig. 3A). A major pipeline was mapped along the bay side of Shelter Island that extends from the channel on the east side of Shelter Island, along the length of Shelter Island, and then bends around the southern end of the island, crosses the channel into Shelter Island Harbor, and continues up to the edge of data coverage near the Point Loma peninsula (Fig. 3B). The pipeline is imaged as a thin continuous feature often observed at the bottom of a topographically low trench (Fig. 3B). A triangular shaped shoal also is located at the southern end of Shelter Island, possibly an extension of fill used to build the island (Fig. 3B). There are also several areas with evidence of anthropogenic sediment re-working. The deepest part of the bay is adjacent to the naval submarine berths (Fig. 3C). Similar round, deep pits are also located near the other major piers around the bay (Fig. 3A, 3B). For example, at the cruise ship terminal, deep pits are observed between the piers and just to the west of the docks the seafloor exhibits semi-circular scours (Fig. 3D). To the north of the cruise ship terminal a ~2 m thick sediment depocenter mantles the most recent dredge surface (Figs. 3D & 4). In Chirp data, the dredge surface is a high amplitude, roughly horizontal reflector. The transparent unit above the dredge surface forms the depocenter, which is bounded on the north and east sides by the steep dredge walls (Fig. 4).

Despite the extensive anthropogenic alterations to the bay, several natural sediment features are also observed. For example, localized bedforms are found throughout the bay. Large-scale bedforms are located near the mouth of the bay, south of the Zuniga Jetty and east of the shipping channel (Fig. 3E). These bedforms are ~20 m wavelength, ~0.2-0.4 m height, are fairly linear, and trend southwest-northeast. They are slightly asymmetrical with the steep stoss side facing towards the southeast. Just north of the jetty on the east side of the channel there is a small patch of roughly symmetrical, large wavelength bedforms within a seagrass bed (~50 m wavelength, ~0.4-0.8 m height) (Fig. 3C). Smaller bedforms are located both on the east and west side of the shipping channel near the bay mouth. East of the shipping channel, ~5-30 m wavelength and ~0.1-0.4 m high, symmetrical bedforms are observed at ~12 m water depth with their axis trending east-west (Fig. 3E). West of the shipping channel, east-west trending, ~4-6 m wavelength, >0.5-0.1 m high symmetrical bedforms are observed south of Ballast Point, in ~6 m water depth (Fig. 3C). The bedforms on the west side of the channel die away approaching the shore at Point Loma where the seafloor exhibits a rougher, blockier character. In chirp profiles across this area, the transgressive surface, represented by a strong, planar reflector, shoals to the west. A thick sediment lens is located adjacent to the dredged channel where the transgressive surface deepens (Fig. 5). A marked increase in sediment thickness occurs where the dip of the transgressive surface changes. The sediment deposit is acoustically transparent and thickens north toward Ballast Point reaching a maximum thickness of ~7 m (Fig. 5). On the surface of the deposit bedforms are ~10-15 m wavelength and ~0.2 m height (Fig. 3C). Another prominent set of bedforms is located between two Coronado Bridge pilings and extends parallel to the

channel ~570 m. The bedforms form a strip with a maximum width of 35 m, with a wavelength of ~5 m and height of ~0.1-0.3 m (Fig. 3F). The axis of the bedforms trends east-west, parallel to the channel, and they appear symmetrical.

Paleochannels are also mapped throughout the bay and offshore Coronado Island and Silver Strand (Fig. 2B). The channels are characterized by a rough, irregular, channel-shaped horizon below the transgressive surface, and are filled with both thinly laminated and transparent to chaotic acoustic packages (Fig. 7).

Tectonics

Faults observed in Chirp data are mapped in Figure 2B. The Spanish Bight fault is mapped as two strands that diverge from Coronado Island to the north. The western strand trends north-south and the east strand trends N25°E. Direct offset of horizons at the fault is difficult to measure, but the fault is identified by highly deformed strata with folded and tilted horizons (Fig. 4). In profiles on the north side of the shipping channel, we observe vertical down to the east offset of the transgressive surface (~0.5 m) and the seafloor (~0.4 m) above at the western fault strand (Fig. 4). Chirp profiles also image the Spanish Bight fault farther south at the edge of the shipping channel (Fig. 8). Here, the western strand appears to diverge upwards into two splays that both offset the seafloor. Horizons are highly deformed by the splays and a small wedge appears rotated (Fig. 8). The eastern strand is mapped out of the channel and offsets horizons below the seafloor down to the east, but does not offset the seafloor. West of the Spanish Bight fault, a previously unmapped fault was identified south of Harbor Island trending roughly north-south (Fig. 4). The fault zone is made up of several splays; offset horizons are identified approximately 2 m below the seafloor.

The seaward extent of some bay faults can be mapped offshore Coronado Island and the Silver Strand. For example, a splay of the Spanish Bight fault can be traced laterally offshore for ~7 km with a trend of ~N14°E (Fig. 9). The fault offsets the transgressive surface with a down to the east sense of slip. Maximum offset is approximately 1.2 m at a minimum water depth of ~16.7 m. At the southern extent, the fault appears to border the Cretaceous Rosario Group extending south from Point Loma. Offshore the paleochannels appear to be fault controlled (Fig. 7).

Three continuous fault strands are mapped as part of the Coronado fault zone (Fig. 10). The northern and central strands are subparallel and trend N30°E while the southern strand trends north-south (Fig. 2B). The northern strand is identified by downward folded horizons towards the fault (Fig. 10). The uppermost deformed horizon is ~2.6 m below the seafloor. The central strand is also marked by deformed horizons and exhibits some down to the west vertical offset. The depth to the most recent offset is difficult to define because of the extensive deformation, but the seafloor does not appear offset. Vertical offset is also observed on the southernmost strand. Offset is observed as both down to the east and down to the west with the youngest offset horizon ~1.6 m below the seafloor. Maximum observed offset at the strand is ~3.7 m.

Previous mapping of the Silver Strand fault through the bay have the fault oriented roughly north-south (Ref – Kennedy??). In Chirp data, two continuous strands are mapped in this vicinity, but they trend N58°W (Figs. 2B &11). There appears to be slight vertical offset on the fault, but it is primarily identified by folding and deformation. Additionally, in the vicinity of the Silver Strand fault zone, a high amplitude, chaotic acoustic unit obscures detailed imaging below. The youngest offset observed is ~ 1 m

below the seafloor. We also observe complex faulting in the vicinity of the Coronado Bridge with two distinct, continuous fault strands that trend N32°W. These faults also exhibit dip-slip motion and most recent offsets occur at variable depths. Offset on these strands reaches ~5 m (Fig. 12).

Biological

We observe variations in the density and patterns of seagrass and kelp forest within areas of San Diego Bay. Figure 3C illustrates the acoustic signal produced by these plants. Although diving was not performed as part of this effort, some of the vegetation was examined from the vessel and correlated to the bathymetric signals in real time. Additionally, comparisons between bathymetric signals were correlated to previously mapped seagrass and kelp distributions to build confidence in identifying the plants imaged in the bathymetric and backscatter data (Parnell, personal communication Reference from Todd??). East of Point Loma, backscatter data images two types of kelp plants; pterygophora and feather boa kelp. The pterygophora kelp was imaged as semi-circular bright spots while the feather boa kelp was imaged as long thin bright spots. These kelp plants are only located close to Point Loma and are not observed elsewhere in the bay.

Seagrass is observed in locations throughout the bay, primarily in shallow areas. A large seagrass bed is located between the shipping channel and Zuniga Jetty (Fig. 3C). In the bathymetry data, the seagrass is imaged as a rough seafloor that reaches up to 0.6 m above surrounding smooth seafloor. The bed grows from the shallowest depths out to ~ 5.5 m water depth. Within the regional distribution of seagrass there are some internal bare patches (Fig. 3C). One patch is tongue shaped oriented roughly east-west and

located adjacent to the Zuniga Jetty at ~4 m water depth. The other patch is north of the jetty in ~3 m water, is also tongue shaped, and is filled with ~50 m wavelength bedforms. Within the bare patch, there are east-west oriented bedforms with ~50 m wavelength and slight asymmetry; the lee face is along the north side of the bedforms (Fig 3C).

DISCUSSION

Sediment

Much of San Diego Bay has been anthropogenically altered; its shorelines sediment distribution, and seafloor morphology. The sharp edges of dredged channels, linear cable trenches, and scour marks typical of the dredging process are all observed in the bay. Furthermore, anthropogenic forcing in the bay appears to play an important role in circulation patterns, sediment redistribution, and habitat patchiness.

The largest anthropogenic redistribution of sediment in the bay appears to be associated with the cruise ship terminal and naval submarine base. At the cruise ship terminal, seafloor roughness and semi-circular patterns on the seafloor may be associated with propeller motion scraping and stirring up sediment. The re-suspended sediment is then re-deposited to the north in the corner of the dredged area because as the cruise ships exit the pier they turn clockwise and shunt all the re-suspended sediment northward (Fig. 3D and Fig. 4). The smooth seafloor on top of the thick sediment package indicates a primarily depositional environment contrasting with the scoured and rough erosional surface just to the south adjacent to the terminals (Fig. 3D). The most recent dredging occurred in 2004, and ~2 m of sediment has been deposited above the dredge surface since that time (Fig. 4).

The deepest point in San Diego Bay, adjacent to the naval submarine bays at Ballast Point was likely created by submarine operations eroding and re-suspending sediment (Fig. 3C). Some of this sediment would then become entrained in tidal currents and re-deposited elsewhere. We interpret the thick sediment deposit south of Ballast Point to be a constructional drift deposit created by swift tidal pumping through the narrow channel between Ballast Point and Coronado Island interacting with more quiescent water as the flow expands laterally just south of Ballast Point (Fig. 5). Some of the sediment entrained in the water column by the C-Tractor tugs towing the submarines likely contributes to this deposit. The diminishing thickness to the south indicates the deposit formed more on the ebb than the flood tide, and the topography of the deposit indicates it is constructional in nature (Figs. 3C and 5). .

Other anthropogenic alterations are important for considering circulation patterns within the bay. For example, the pipeline and shoal at the mouth of Shelter Island harbor could be playing an important role in bay circulation (Fig. 3B); inhibiting circulation in and out of Shelter Island harbor. Hull paint and the lack of tidal flushing in and out of the Shelter Island harbor would contribute to the build-up of high concentrations of copper in the water and surficial sediment (Ref. Helly?).

The bedforms located under and south of the Coronado Bridge appear tidally controlled (Fig. 3F). The symmetric shape is consistent with an oscillatory tidal current. The isolation of the bedforms in a thin ribbon is likely associated with the predominant path of large ships through the bridge pilings. Large cargo and military ships generally go under the span of the Coronado Bridge along the northern edge of the dredged channel; a

path marked by bedforms. The propeller swash from the ships could be winnowing out fine grain sediments, leaving behind sands that more readily form bedforms.

South of Ballast Point, the transgressive surface shoals from the shipping channel towards Point Loma and appears to control the morphological features on the seafloor (Fig. 5). Closest to Point Loma, rough and blocky seafloor features are found where the transgressive surface appears to subcrop or outcrop near the seafloor. As the transgressive surface plunges to the east, the sediment deposit above thickens, and bedforms on the seafloor are observed. The transgressive surface is ~9 m deep at the channel edge (Fig. 5). Based on the sea level curve of Fairbanks (1989) and the depth of the transgressive surface, inundation occurred at ~5.5 ka. The differential accumulation of sediment near the Embarcadero and south of Ballast Point is very high yet extremely localized (Figs. 3C and 3D).

Tectonics

In some locations, the Spanish Bight fault appears to offset the seafloor (Fig. 8). The offset may be recording real slip on the fault, but could also result from fluid flow along the fault mobilizing unconsolidated sediment. Near the southern shore, offset of the seafloor appears more convincing because of the folded and tilted horizons between the two fault strands (Fig. 8). Towards the northern shore, the western strand offsets the transgressive/dredge surface below the seafloor (Fig. 4). Given the offset of the dredge surface and seafloor, the Spanish Bight fault appears to have been active recently.

The Spanish Bight fault and the newly identified fault (Harbor Island fault) trend north and project out of the bay towards Lindbergh Field (Fig. 4). Prior to permanent re-routing, the San Diego River has historically alternated flow from Mission Valley either

west to Mission Bay or south to San Diego Bay, in the area of modern Harbor Island. Given the dip-slip component on the faults in the area of Harbor Island, these faults may be capable of altering the course of the river by stream capture and may explain the migration of the San Diego River between Mission Valley and San Diego Bay through time.

The 7 km segment of the Spanish Bight fault zone mapped offsore offsets the transgressive surface as shallow as ~16.7 m below seafloor (Fig. 9). Based on a eustatic sea level curve and the assumption that the offset post-dated the formation of the transgressive surface, this constrains the age of the most recent event to be younger than 7.5 ka (Fairbanks, 1989). The 1.2 m offset of the transgressive surface is overlain by mobile Holocene sands, which would likely relax and thus erase any seafloor offset. Therefore, the most recent event on this strand may be younger than 7.5 ka. If the maximum 1.2 m offset resulted from one earthquake, the slip rate on this fault is ~0.16 mm/yr and the potential magnitude of the most recent event was ~M6.35 (7 km length and 15 km depth of fault zone -Wells and Coppersmith, 1994). This may be an underestimate because it only accounts for the vertical offset on a transtensional fault.

The shallow depths of offset on the Coronado and Silver Strand faults also suggest that these faults are active in the Holocene and vertical offsets demonstrates a component of dip-slip motion (transtension) on the faults. The transtensional faults also may play an important role in groundwater transport and flux of freshwater to the bay.

Biological

Light availability (related to depth and water clarity) and nutrient supply are the most important controls on seagrass distribution, but substrate characteristics also

influence seagrass habitats. Patterns in seagrass distribution appear controlled by sediment processes in some areas of the bay. For example, west of Zuniga Jetty, we observe patchiness in seagrass habitat that does not appear to be depth or nutrient controlled because the patches occur within a regionally continuous zone that is mostly covered with seagrass. A bare patch located adjacent to Zuniga Jetty may be related to sediment spilling through the jetty from the east that constantly blankets the area (Fig. 3C). A bare patch farther north from the jetty is characterized by bedforms suggesting this zone may have coarser sediment than surrounding areas or increased current-control. The bare patch is just south of the narrowest part of the mouth of the bay between Ballast Point and Coronado Island, and adjacent to a slight outward jog in the Coronado Island shoreline with a groin. Tidal currents through the narrow passage would be enhanced and could potentially winnow out fine sediments in the seagrass free patch (Fig. 3C).

On the east side of Point Loma, patterns in kelp growth appear controlled by the shoaling of the transgressive surface towards the peninsula (Figs. 3C and 5). As the trangressive surface shoals, the younger sediment package above thins and exposes the underlying hardgrounds that is rockier. Multibeam data indicates that hardground outcrops at the seafloor are not as continuous as on the west side of Point Loma, which may result in the different ecosystem characteristics observed in the major Point Loma kelp forest offshore (Figs 1 and 9).

CONCLUSIONS

Anthropogenic forcing plays a major role in sediment processes and consequent morphology in San Diego Bay. With minimal terrestrial input, shipping activities in the bay appear to be the major driver of sediment reworking and differential deposition. Symmetric bedforms throughout much of the bay are consistent with oscillatory tidal pumping, which is an important process for bay circulation and flushing. Faults mapped in the bay appear transtensional and several appear active in the Holocene. Dip slip motion on bay faults, in particular the Spanish Bight and Harbor Island faults could play an important role in groundwater flow and may have altered the course of the San Diego River by stream capture. Furthermore, paleochannels and faulting through the Silver Strand could create weak zones that could lead to breakthrough during the rapid sea level rise and astronomical high tides. The geology of the bay, both natural and anthropogenic has important links to seagrass and kelp habitats.

Future work needs to be conducted to understand better the impact of anthropogenic structures and sediment re-working on bay circulation and contamination. Dating of sediments within the bay would provide insights into the earthquake history on active faults to assess seismic risk to the cities of San Diego and Coronado. Modeling of predicted future sea level rise using bathymetry and Chirp data presented here also would elucidate potential hazards and assist in preparing for future impacts. Furthermore, this study provides a baseline for future work on seagrass and kelp habitats in the bay, which will be important for ecosystem management plans in response to rapid sea level and increase storminess.

REFERENCES CITED

Astiz, L., and Shearer, P.M., 2000, Earthquake locations in the inner Continental Borderland, offshore southern California: Bulletin of the Seismological Society of America, v. 90, no. 2, p. 425-449.

Basile, C., and Brun, J.P., 1998, Transtensional faulting patterns ranging from pull-apart basins to transform continental margins; an experimental investigation: Journal of Structural Geology, v. 21, no. 1, p. 23-37.

Bell, S.S., Robbins, B.D., and Jensen, S.L., 1999, Gap dynamics in a seagrass landscape: Ecosystems, v. 2, no. 6, p. 493-504.

Canada, L.A., 2006, "Sitting on the Dock of the Bay:" 100 years of photographs from the San Diego Historical Society: The Journal of San Diego History, San Diego Historical Society Quarterly, v. 52, no. 1 & 2, Eds. Engstrand, I.H.W. and McClain, M.

Chadwick, D.B., and Largier, J.L., 1999, The influence of tidal range on the exchange between San Diego Bay and the ocean: Journal of Geophysical Research, v. 104, no. C12, p. 29,885-829,899.

Daniell, J.J., Harris, P.T., Hughes, M.G., Hemer, M., and Heap, A., 2008, The potential impact of bedform migration on seagrass communities in Torres Strait, northern Australia: Continental Shelf Research, v. 28, no. 16, p. 2188-2202.

Delgadillo-Hinojosa, F., Zirino, A., Holm-Hansen, O., Hernandez-Ayon, J.M., Boyd, T.J., Chadwick, B., and Rivera-Duarte, I., 2008, Dissolved nutrient balance and net ecosystem metabolism in a Mediterranean-climate coastal lagoon: San Diego Bay: Estuarine Coastal and Shelf Science, v. 76, p. 594-607.

Duarte, C.M., 2002, The future of seagrass meadows: Environmental Conservation, v. 29, no. 2, p. 192-206.

Fairbanks, R.G., 1989, A 17,000-year glacio-eustatic sea level record; influence of glacial melting rates on the Younger Dryas event and deep-ocean circulation: Nature, v. 342, no. 6250, p. 637-642.

Fonseca, M.S., Kenworthy, W.J., and Thayer, G.W., 1998, Guidelines for the conservation and restoration of seagrasses in the United States and adjacent waters: National Oceanic and Atmospheric Administration (NOAA) Coastal Ocean Office.

Hart, M.W., 1974, Radiocarbon Ages Of Alluvium Overlying La-Nacion Fault, San-Diego, California: Geological Society Of America Bulletin, v. 85, no. 8, p. 1329-1332.

Hemminga, M.A., and Duarte, C.M., 2000, Seagrass Ecology, Cambridge, Cambridge University Press.

Henkart, P., 2003, SIOSEIS software. Scripps Institution of Oceanography, La Jolla, California. http://sioseis.ucsd.edu.

Hine, A.C., Evans, M.W., Davis, R.A., and Belknap, D.F., 1987, Depositional response to seagrass mortality along a low-energy, barrier-island coast, West-central Florida: Journal of Sedimentary Petrology, v. 57, no. 3, p. 431-439.

Intergovernmental Panel on Climate Change (IPCC), 2007, The Physical Science Basis: Contribution of Working Group I to the Fourth Assessment Report of the Intergovernmental Panel on Climate Change, Eds. S. Solomon et al., Cambridge University Press, Cambridge.

Katzman, R., ten Brink, U.S., and Lin, J., 1995, Three-dimensional modeling of pull-apart basins; implications for the tectonics of the Dead Sea Basin: Journal of Geophysical Research, v. 100, no. B4, p. 6295-6312.

Kennedy, M.P., and Clarke, S.H., 1999, Analysis of late Quaternary faulting in San Diego Bay and hazard to the Coronado Bridge: California Division of Mines and Geology Open-File Report, v. 97-10A.

Kennedy, M.P., and Welday, E.E., 1980, Recency and character of faulting offshore metropolitan San Diego, California: California Division of Mines and Geology.

Koch, E.M., 2001, Beyond light: Physical, geological, and geochemical parameters as possible submersed aquatic vegetation habitat requirements: Estuaries, v. 24, no. 1, p. 1-17.

Largier, J.L., 1995, San Diego Bay Circulation - A study of the circulation of water in San Diego Bay for the purpose of assessing, monitoring and managing the transport and potential accumulation of pollutants and sediment in San Diego Bay.

Largier, J.L., Hollibaugh, J.T., and Smith, S.V., 1997, Seasonally Hypersaline Estuaries in Mediterranean-climate Regions: Estuarine, Coastal and Shelf Science, v. 45, p. 789-797.

Legg, M.R., 1985, Geologic structure and tectonics of the inner continental borderland offshore northern Baja California, Mexico: University of California Santa Barbara Ph.D. thesis.

Lindvall, S.C., and Rockwell, T.K., 1995, Holocene activity of the Rose Canyon fault zone in San Diego, California: Journal of Geophysical Research, v. 100, no. B12, p. 24,121-124,132.

Magistrale, H., 1993, Seismicity of the Rose Canyon fault zone near San Diego, California: Bulletin of the Seismological Society of America, v. 83, no. 6, p. 1971-1978.

Maloney, J.M., Driscoll, N.W., Kent, G.M., and Brothers, D.S., in prep., Segmentation and step-overs along strike slip fault systems in the inner California borderlands: Implications for fault architecture and basin formation.

Marba, N., and Duarte, C.M., 1995, Coupling of seagrass (Cymodocea-nodosa) patch dynamics to subaqueous dune migration: Journal of Ecology, v. 83, no. 3, p. 381-389.

Marshall, M., 1989, Detailed gravity studies and the tectonics of the Rose Canyon--Point Loma--La Nacion Fault System, San Diego, California: Proceedings, Workshop on "The seismic risk in the San Diego region: Special focus on the Rose Canyon Fault system," June 29-30. Ed. Roquemore, G., p. 80-99.

Masters, P.M., 2006, Holocene sand beaches of Southern California: ENSO forcing and coastal processes on millennial scales: Palaeogeography, Palaeoclimatology, Palaeoecology, v. 232, no. 1, p. 73-95.

Mazor, R.D. and Schiff, K., 2007a, Surface water ambient monitoring program (SWAMP) report on the Otay Hydrologic Unit: Technical Report 527, prepared for the California Regional Water Quality Control Board, San Diego Region (Region 9). Southern California Coastal Water Research Project.

Mazor, R.D. and Schiff, K., 2007b, Surface water ambient monitoring program (SWAMP) report on the Pueblo San Diego Hydrologic Unit: Technical Report

527, prepared for the California Regional Water Quality Control Board, San Diego Region (Region 9). Southern California Coastal Water Research Project.

Mazor, R.D. and Schiff, K., 2007c, Surface water ambient monitoring program (SWAMP) report on the Sweetwater Hydrologic Unit: Technical Report 527 prepared for the California Regional Water Quality Control Board, San Diego Region (Region 9). Southern California Coastal Water Research Project.

McClay, K., and Dooley, T., 1995, Analogue models of pull-apart basins: Geology, v. 23, no. 8, p. 711-714.

Orth, R.J., Carruthers, T.J.B., Dennison, W.C., Duarte, C.M., Fourqurean, J.W., Heck, K.L., Hughes, A.R., Kendrick, G.A., Kenworthy, W.J., Olyarnik, S., Short, F.T., Waycott, M., and Williams, S.L., 2006, A global crisis for seagrass ecosystems: Bioscience, v. 56, no. 12, p. 987-996.

Peng, J., and Zeng, E.Y., 2007, An integrated geochemical and hydrodynamic model for tidal coastal environments: Marine Chemistry, v. 103, no. 1-2, p. 15-29.

Pfeffer, W.T., Harper, J.T., and O'Neel, S., 2008, Kinematic constraints on glacier contributions to 21st-century sea-level rise: Science, v. 321, p. 1340-1343.

Pourade, R.F., 1960, The Explorers 1492-1774, Union-Tribune Publishing Company, Copley Press.

Rahmstorf, S., 2007, A semi-emperical approach to projecting future sea-level rise: Science, v. 315, p. 368-370.

Rambo, C.E. and Speidel, W.C., 1969, A case study of estuarine sedimentation in Mission Bay-San Diego Bay, California, Prepared for U.S. Department of the

Interior, Federal Water Pollution Control Administration, Contract no. 14-12-425. Marine Advisers, Inc., La Jolla, California.

Rockwell, T., 2010, The Rose Canyon Fault Zone in San Diego, Fifth International Conference on Recent Advances in Geotechnical Earthquake Engineering and Soil Dynamics and Symposium in Honor of Professor I.M. Idriss: San Diego, California.

Ryan, H.F., Conrad, J.E., Paull, C.K., and McGann, M., 2012, Slip rate on the San Diego Trough Fault Zone, Inner California Borderland, and the 1986 Oceanside Earthquake Swarm Revisited: Bulletin of the Seismological Society of America, v. 102, no. 6, p. 2300-2312.

United States Fish and Wildlife Service (USFWS), 2006, San Diego Bay National Wildlife Refuge, Sweetwater Marsh and South San Diego Bay Units: Final Comprehensive Conservation Plan and Environmental Impact Statement Summary. Downloaded 5/6/2011 from http://www.fws.gov/sandiegorefuges/new/ccp/ccp.htm.

Short, F.T., and Wyllie-Echeverria, S., 1996, Natural and human-induced disturbance of seagrasses: Environmental Conservation, v. 23, no. 1, p. 17-27.

Waycott, M., Duarte, C.M., Carruthers, T.J.B., Orth, R.J., Dennison, W.C., Olyarnik, S., Calladine, A., Fourqurean, J.W., Heck, K.L., Hughes, A.R., Kendrick, G.A., Kenworthy, W.J., Short, F.T., and Williams, S.L., 2009, Accelerating loss of seagrasses across the globe threatens coastal ecosystems: Proceedings of the National Academy of Sciences of the United States of America, v. 106, no. 30, p. 12377-12381.

Wells, D.L., and Coppersmith, K.J., 1994, New Empirical Relationships among Magnitude, Rupture Length, Rupture Width, Rupture Area, and Surface Displacement: Bulletin of the Seismological Society of America, v. 84, no. 4, p. 974-1002.

Wu, J.E., McClay, K., Whitehouse, P., and Dooley, T., 2009, 4D analogue modelling of transtensional pull-apart basins: Marine and Petroleum Geology, v. 26, p. 1608-1623.

FIGURES

Figure 1. Regional map of San Diego showing major fault zones and morphologic features. Major fault zones are labeled.

Figure 2A. Map of San Diego Bay showing collected bathymetry data, Chirp track lines (white), previously mapped faults (green), and faults mapped in this study (black). Abbreviations: HIF – Harbor Island Fault; SBF – Spanish Bight Fault; CF – Coronado Fault; SSF – Silver Strand Fault. 2B. Map of San Diego Bay showing collected bathymetry data, Chirp track lines (white), and locations of Chirp figures shown in the paper. HIF – Harbor Island Fault

Figure 3. Map of San Diego Bay showing collected bathymetry data and locations of blow-up figures.

A. Bathymetry illustrating the morphology of the shipping channel, dredge scours, cross-channel trenches, and deep pits interpreted to result from shipping traffic.

B. Bathymetry from near Shelter Island showing the triangular shoal extending north from the island, the long pipeline, which runs along the entire length of the island, and deep pits associate with the Scripps Marine Facility.

C. Bathymetry from near the mouth of San Diego Bay illustrating several features described in detail in the text.

D. Bathymetry from near the cruise ship terminal showing sediment scour and re-working.

E. Bathymetry from the mouth of the bay showing several bedforms of various scales.

F. Bathymetry near Coronado Bridge showing a ribbon of bedforms.

Figure 4. Chirp profile imaging deformation on the newly mapped Harbor Island fault (HIF) and the Spanish Bight fault (SBF). In this region, the SBF appears to offset the dredge surface and the seafloor over the western strand. Also imaged is the sediment lens mantling the dredged surface north of the cruise ship terminals. Location is shown in Figure 2B. Abbreviations: HIF – Harbor Island fault; SBF – Spanish Bight fault.

Figure 5. Chirp profile illustrating the shoaling of the transgressive surface towards Point Loma away from the shipping channel as well as the constructional sediment deposit south of Ballast Point. Location is shown in Figure 2B.

Figure 6. Map showing paleochannels observed in Chirp data (yellow).

Figure 7. Chirp profile offshore the Silver Strand showing paleochannels and strands of the Spanish Bight fault (SBF) and Coronado fault (CF) where they extend offshore. The SBF appears to offset the transgressive surface at this location. Location is shown in Figure 2B. Abbreviations: G – ghost; M – multiple; TS – transgressive surface; SBF – Spanish Bight Fault; CF – Coronado Fault.

Figure 8. Enlarged Chirp profile showing the Spanish Bight fault where the western strand diverges towards the surface into two splays, forming a rotated wedge. The splays

offset the seafloor at the edge of the shipping channel. The eastern strand also deforms horizons outside the channel, but does not appear to offset the seafloor. Location is shown in Figure 2B.

Figure 9. Fence diagram showing Chirp data offshore the Silver Strand with the ~7 km mapped segment of the Spanish Bight fault (dashed red). Yellow is Holocene sediments above the transgressive surface, blue is Cretaceous hardgrounds extending south from Point Loma.

Figure 10. Chirp profile showing three strands of the Coronado Bank fault (dashed). Location is shown in Figure 2B.

Figure 11. Chirp profile showing deformation at the Silver Strand fault (dashed). Location is shown in Figure 2B.

Figure 12. Chirp profile showing offset of horizons on faults just south of Coronado Bridge. Location is shown in Figure 2B.

Figure 1

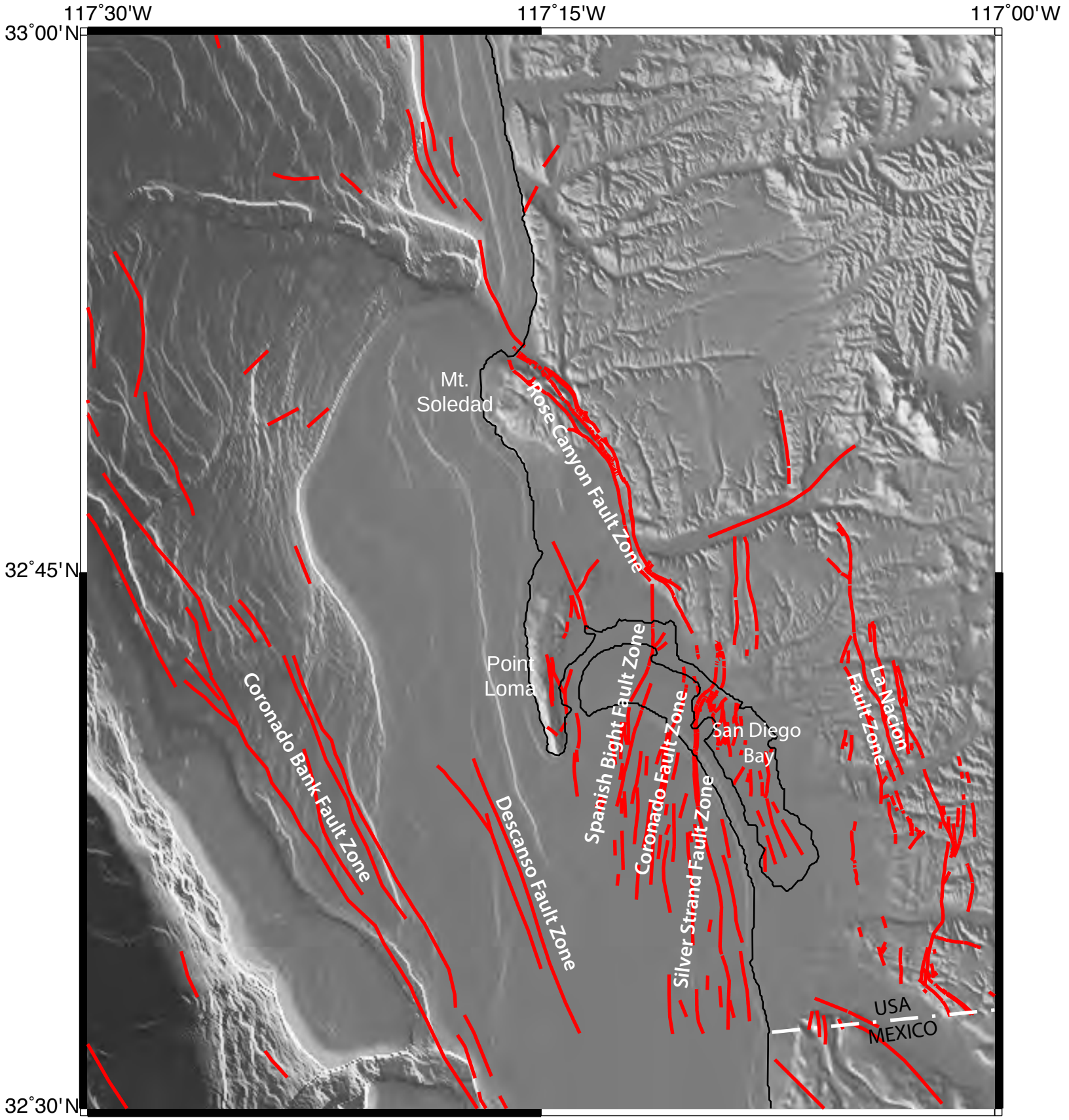
117˚30'W
117˚15'W
117˚00'W
33˚00'N
32˚45'N
32˚30'N
Mt.
Soledad
Rose Canyon Fault Zone
Point
Loma
Coronado Bank Fault Zone
Descanso Fault Zone
Spanish Bight Fault Zone
Coronado Fault Zone
Silver Strand Fault Zone
San Diego
Bay
La Nacion
Fault Zone
USA
MEXICO

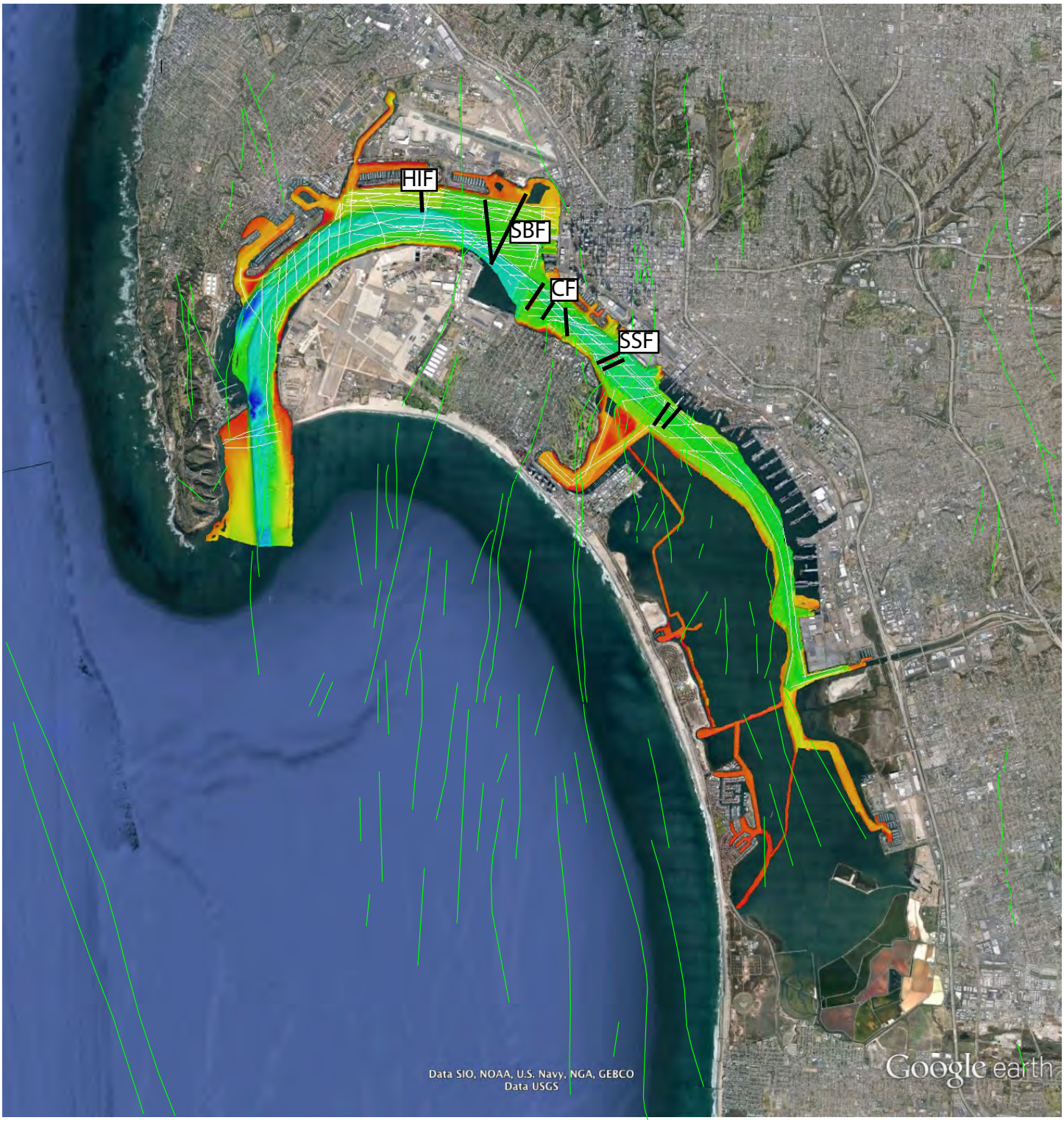

Google earth

miles 6
km 9

Google earth

miles 6
km 9

Figure 3

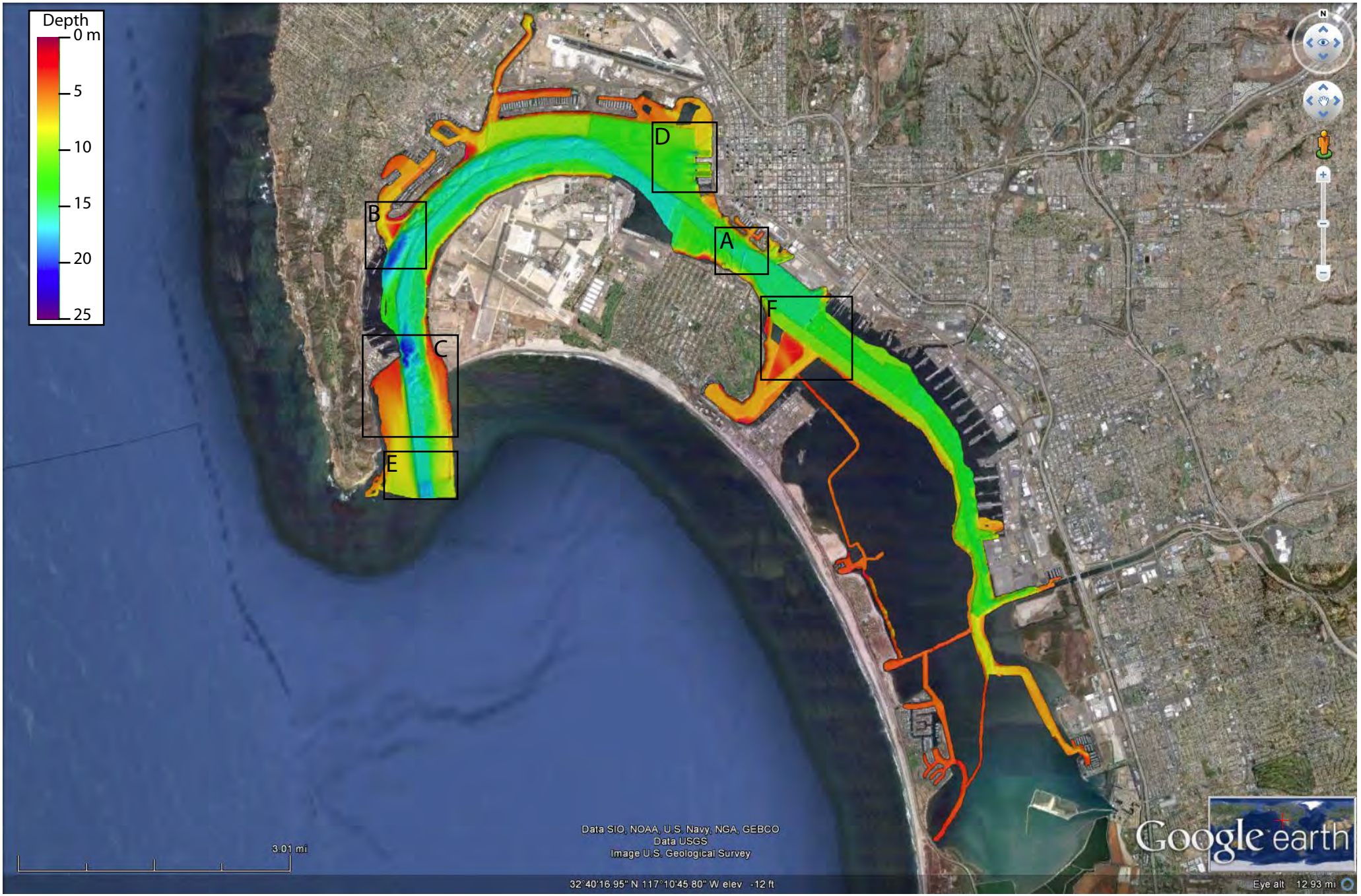
Depth
0 m
5
10
15
20
25
A
B
C
D
E
F
3.01 mi
Data SIO, NOAA, U.S. Navy, NGA, GEBCO
Data USGS
Image U.S. Geological Survey
32°40'16.95" N 117°10'45.80" W elev -12 ft
Google earth
Eye alt 12.93 mi

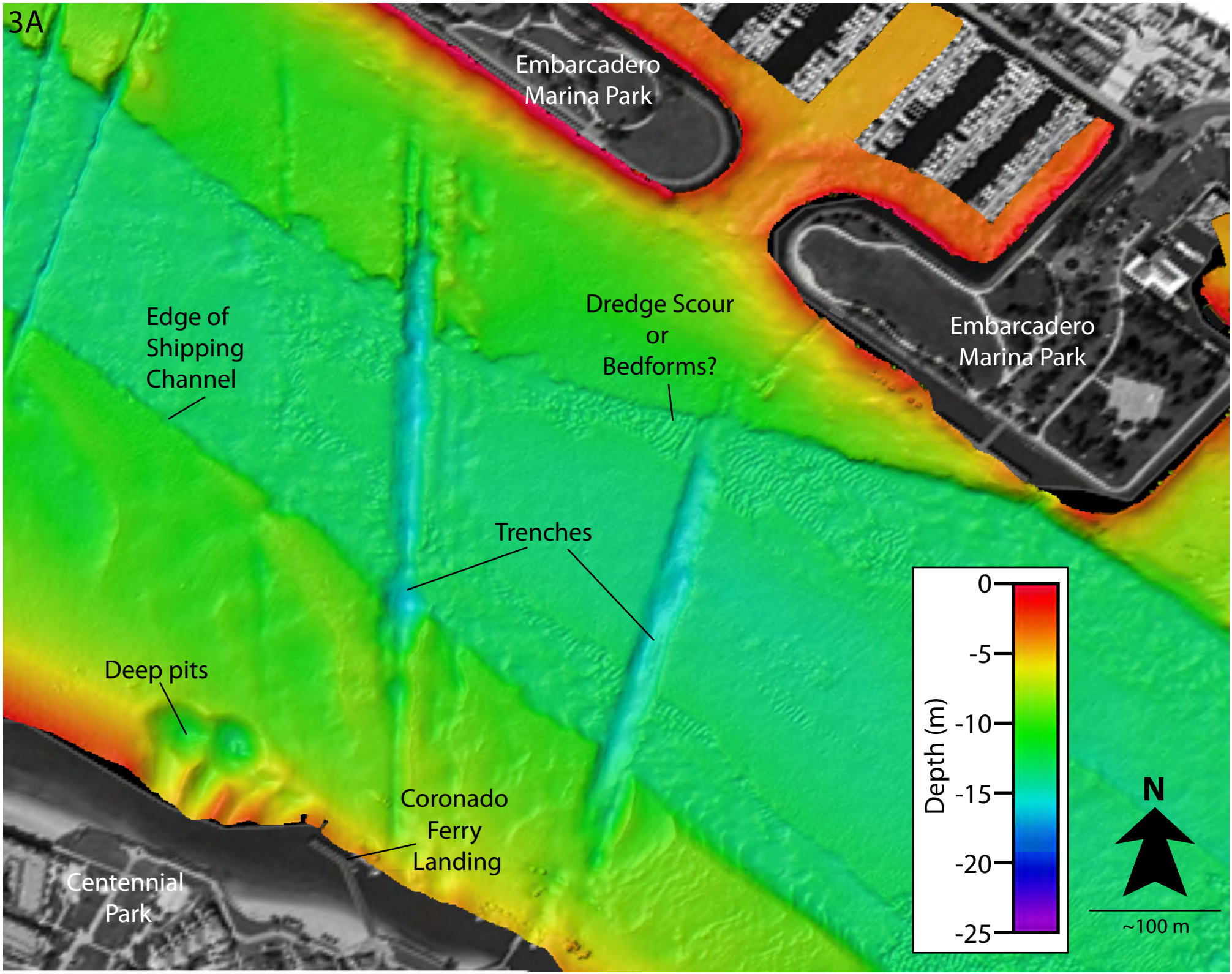
3A
Embarcadero
Marina Park
Edge of
Shipping
Channel
Dredge Scour
or
Bedforms?
Embarcadero
Marina Park
Trenches
Deep pits
Coronado
Ferry
Landing
Centennial
Park
0
-5
-10
-15
-20
-25
Depth (m)
N
~100 m

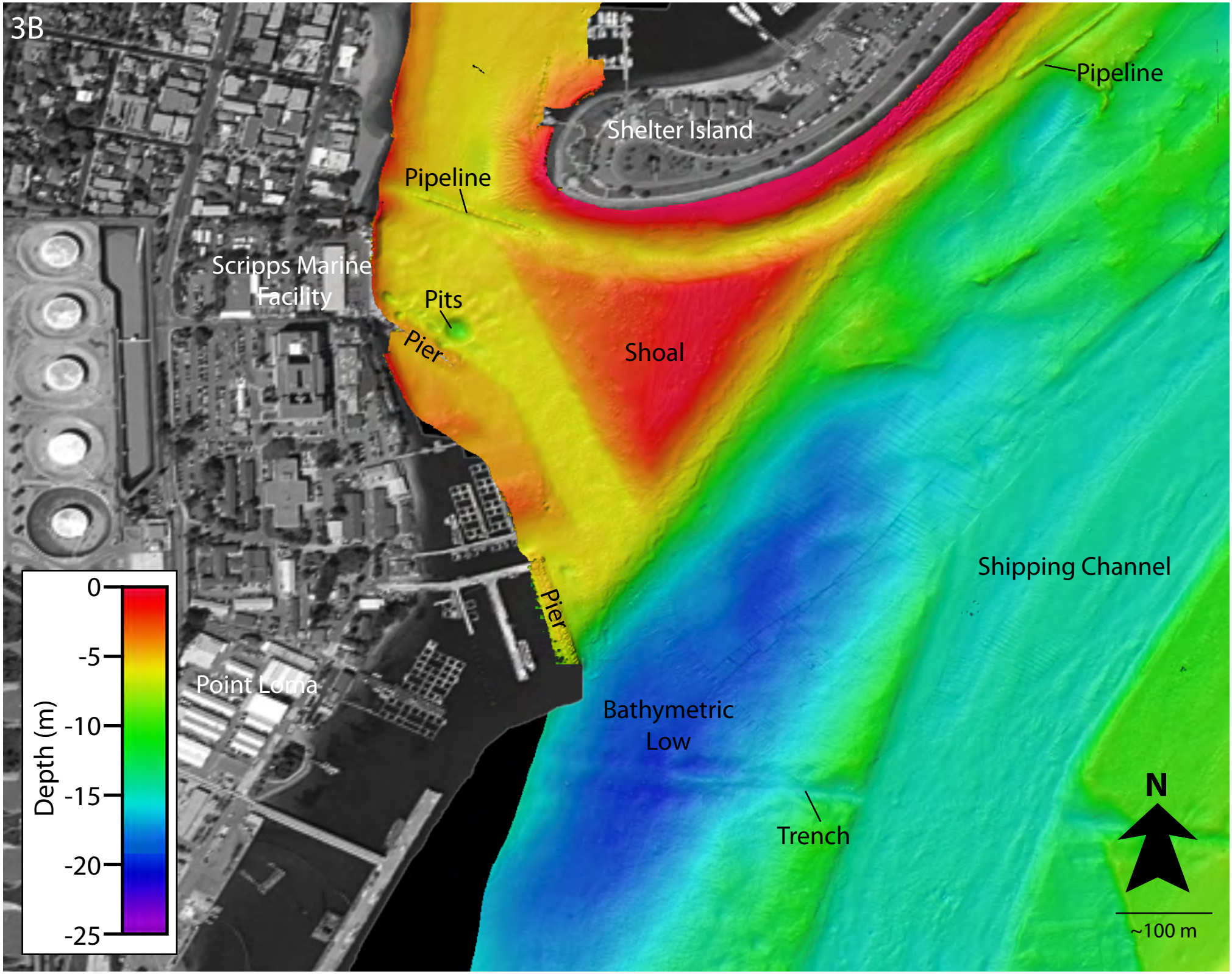
3B
Pipeline
Shelter Island
Pipeline
Scripps Marine Facility
Pits
Pier
Shoal
Shipping Channel
Pier
Point Loma
Bathymetric Low
Trench
Depth (m)
0
-5
-10
-15
-20
-25
N
~100 m

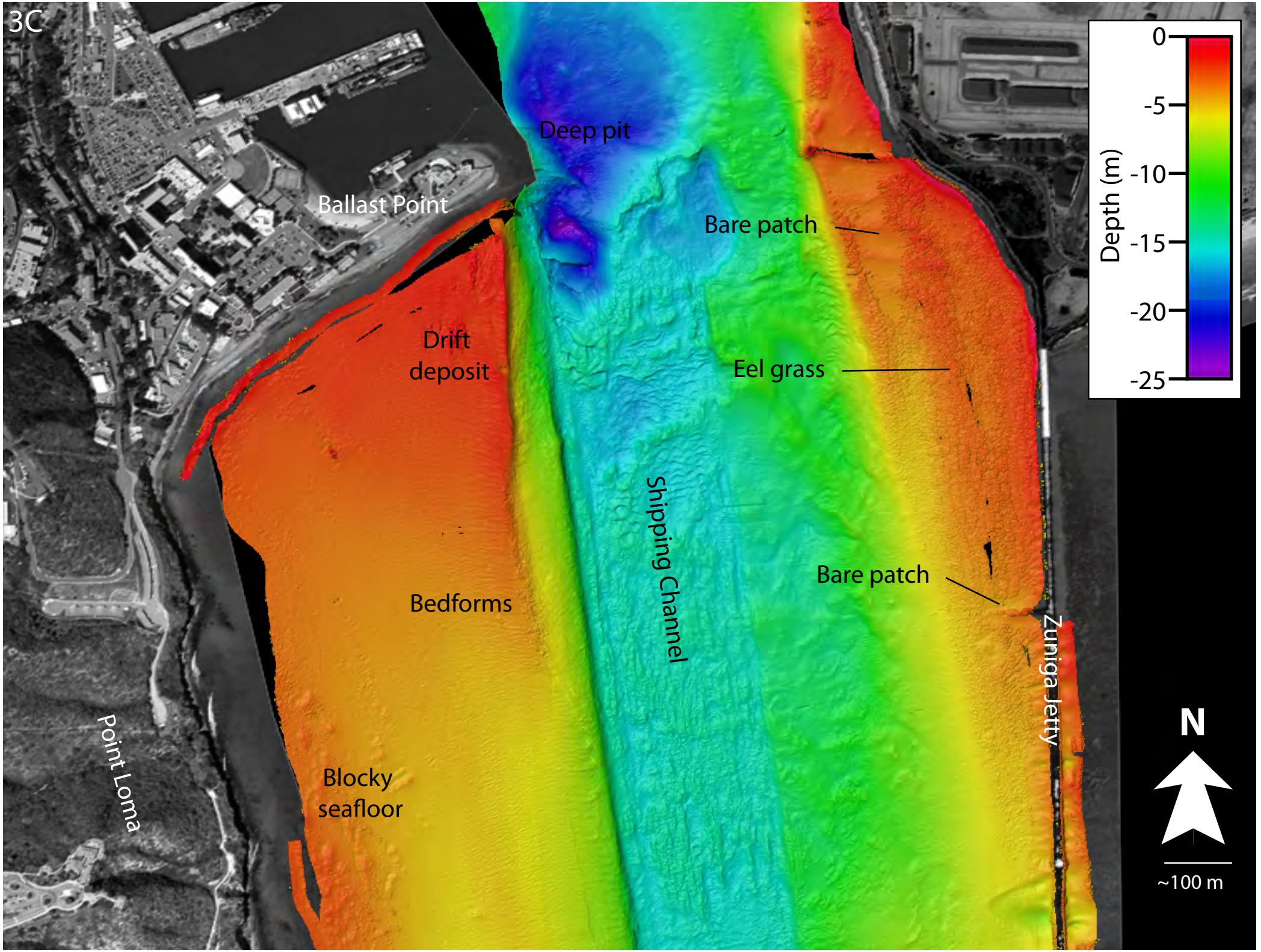
3C
Deep pit
Ballast Point
Bare patch
Drift deposit
Eel grass
Shipping Channel
Bare patch
Bedforms
Zuniga Jetty
Point Loma
Blocky seafloor
Depth (m)
0
-5
-10
-15
-20
-25
N
~100 m

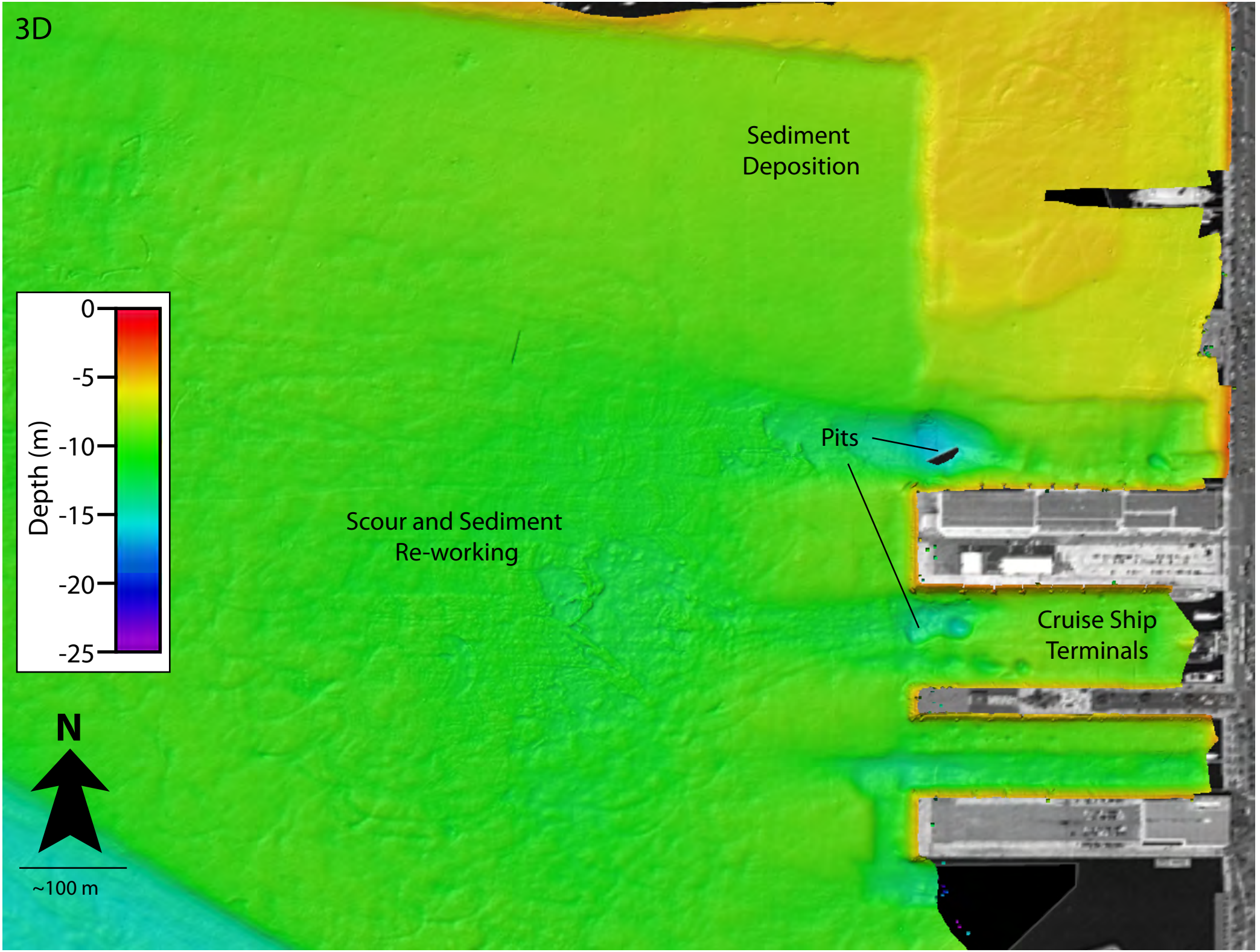
3D
Sediment
Deposition
Pits
Scour and Sediment
Re-working
Cruise Ship
Terminals
Depth (m)
0
-5
-10
-15
-20
-25
N
~100 m

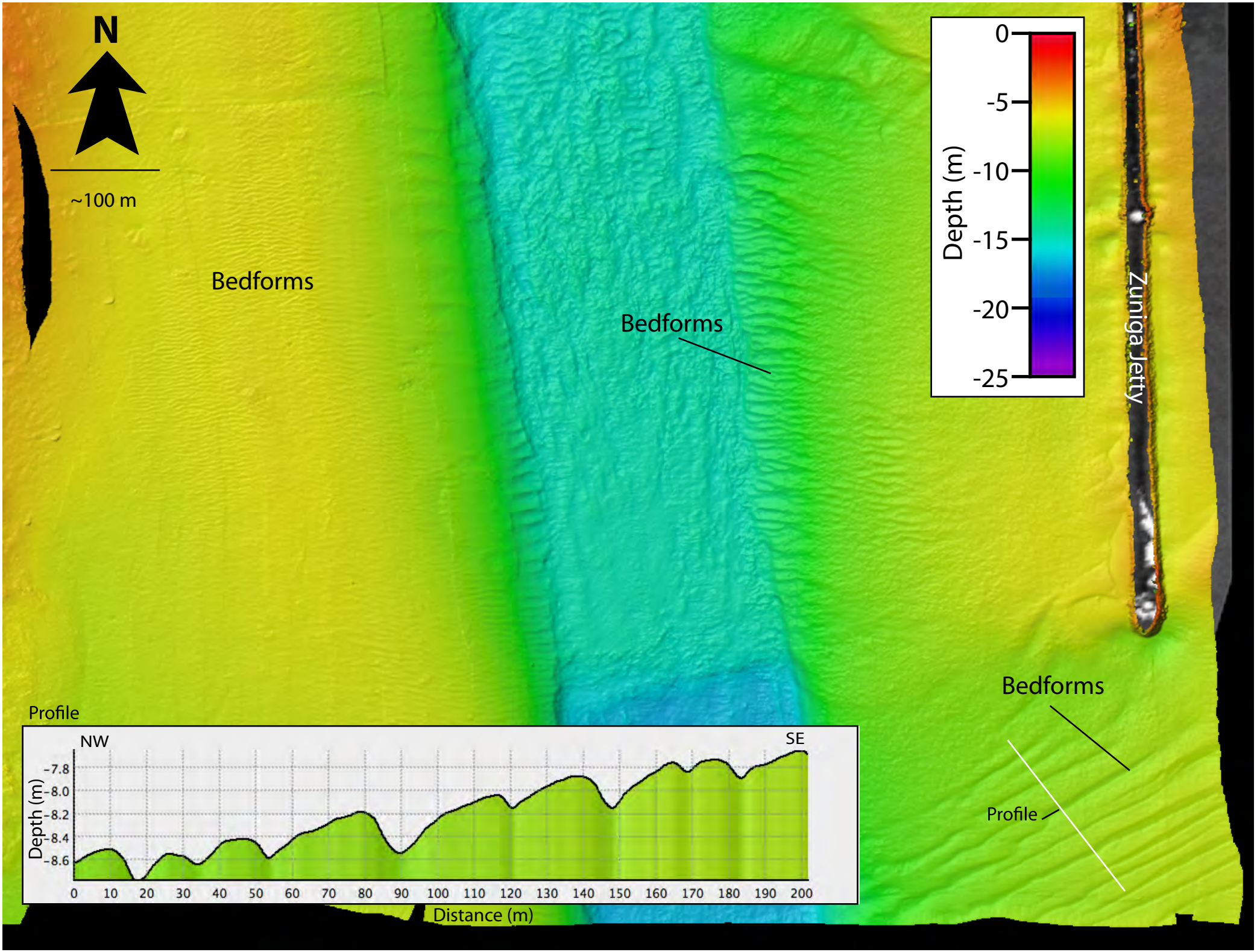
N
~100 m
Bedforms
Bedforms
Depth (m)
0
-5
-10
-15
-20
-25
Zuniga Jetty
Bedforms
Profile
Profile
NW
SE
Depth (m)
-7.8
-8.0
-8.2
-8.4
-8.6
0 10 20 30 40 50 60 70 80 90 100 110 120 130 140 150 160 170 180 190 200
Distance (m)

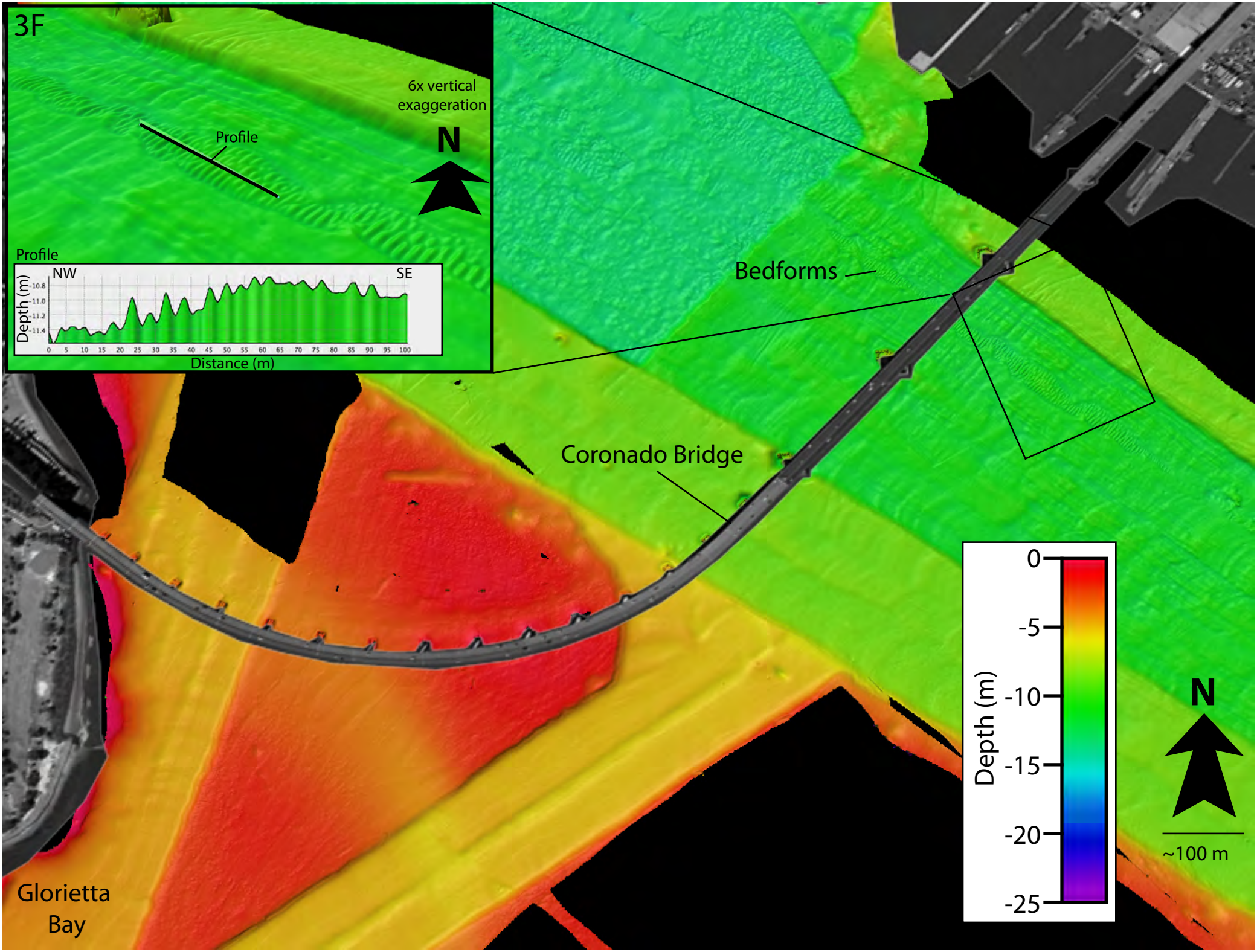
3F
6x vertical exaggeration
Profile
N
Profile
NW
SE
Depth (m)
10.8
11.0
11.2
11.4
0 5 10 15 20 25 30 35 40 45 50 55 60 65 70 75 80 85 90 95 100
Distance (m)
Bedforms
Coronado Bridge
Glorietta Bay
0
-5
-10
-15
-20
-25
Depth (m)
N
~100 m

Figure 4

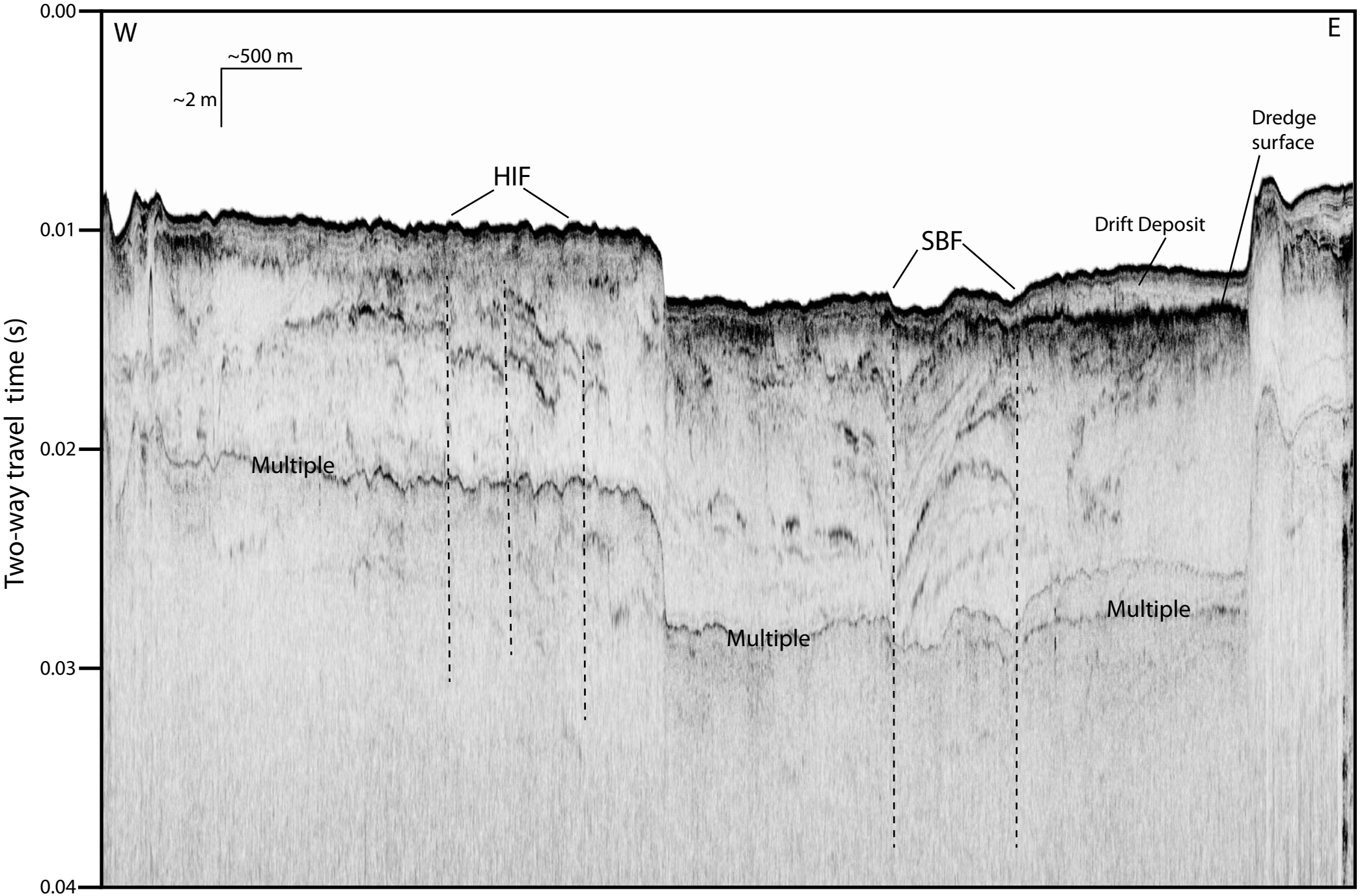
0.00
0.01
0.02
0.03
0.04
Two-way travel time (s)
W
E
~500 m
~2 m
HIF
SBF
Drift Deposit
Dredge surface
Multiple
Multiple
Multiple

Google earth

miles 6
km 9

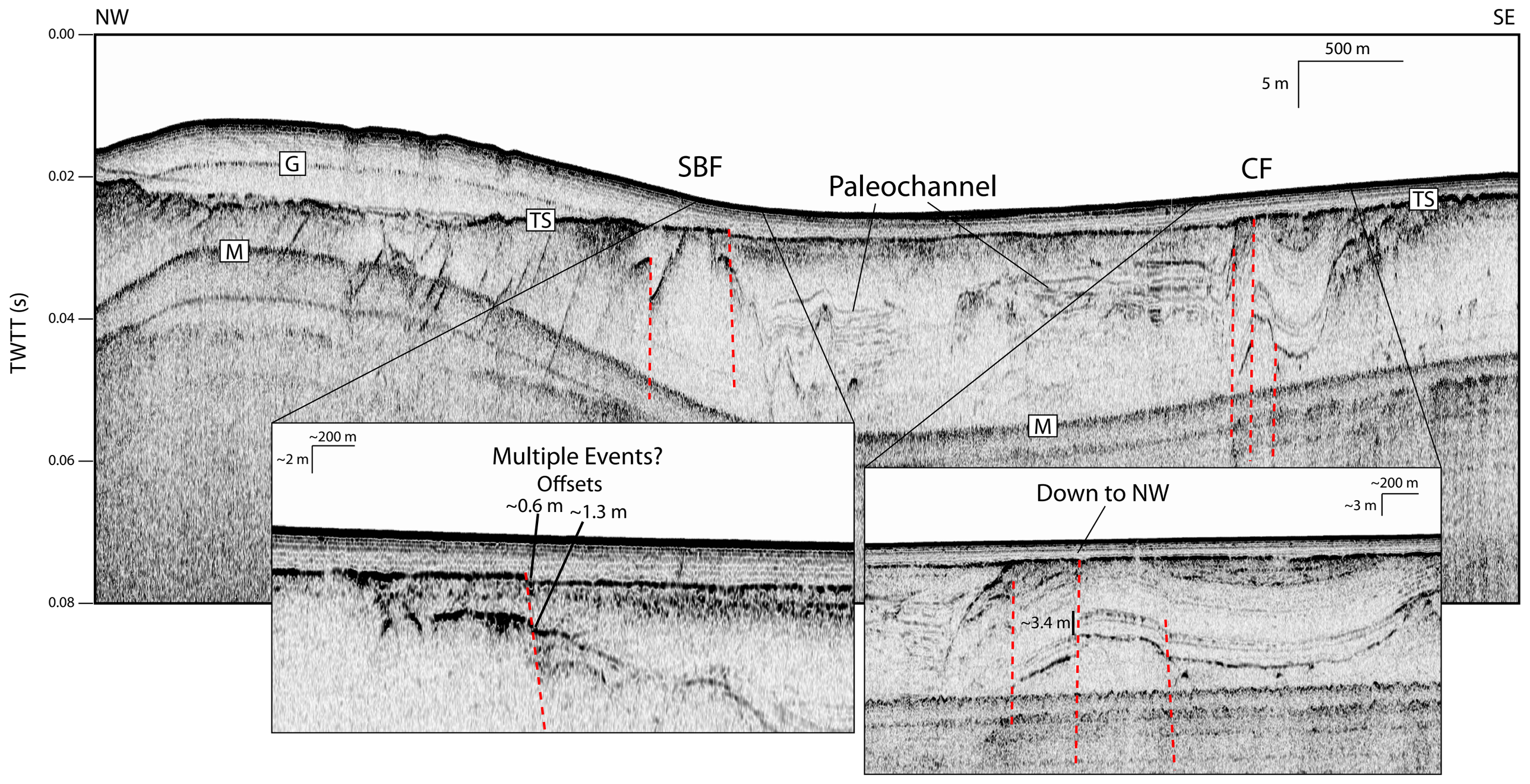
NW
SE
0.00
0.02
0.04
0.06
0.08
TWTT (s)
500 m
5 m
G
M
TS
SBF
Paleochannel
CF
TS
M
~200 m
~2 m
Multiple Events?
Offsets
~0.6 m
~1.3 m
Down to NW
~200 m
~3 m
~3.4 m

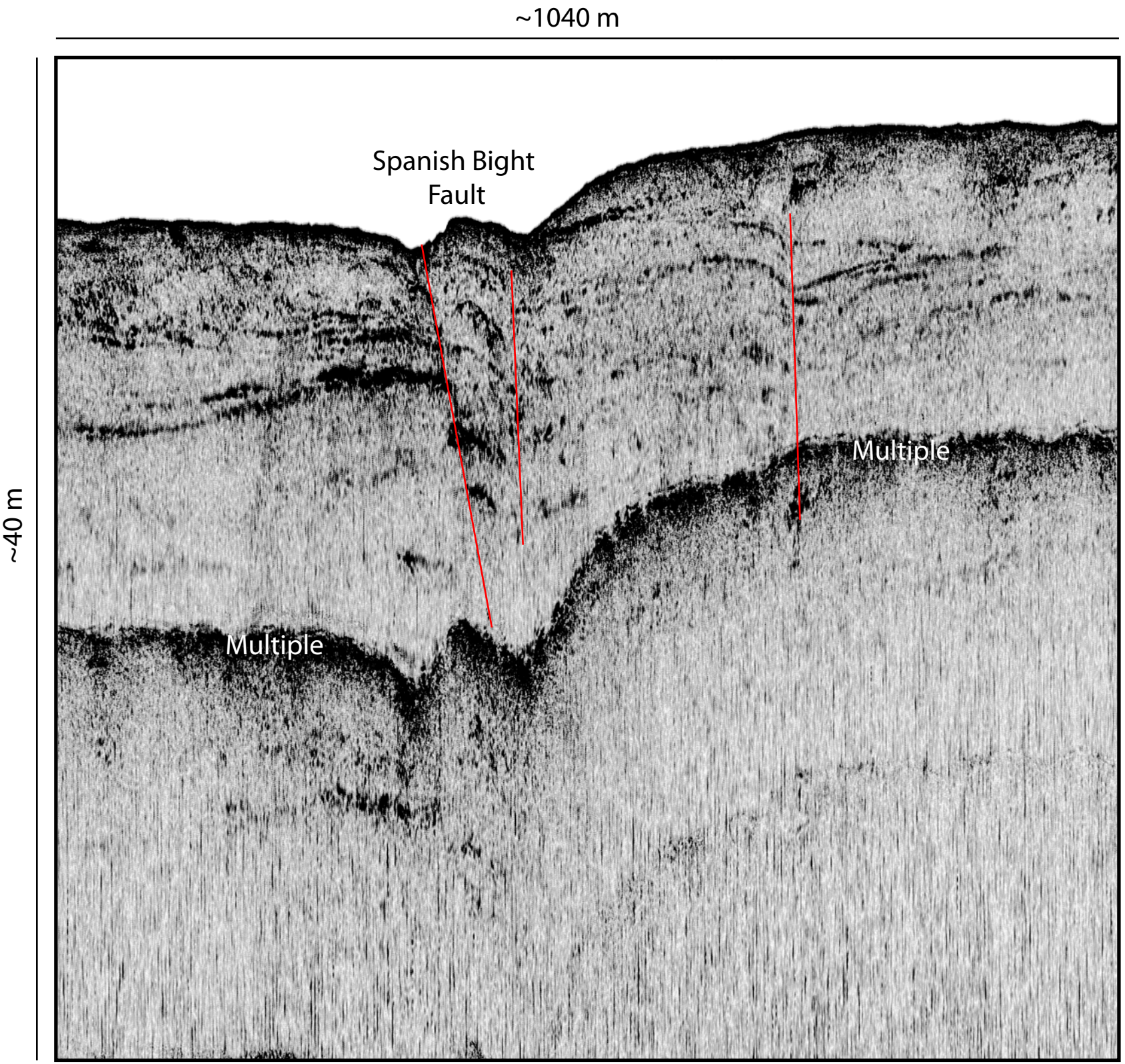
~1040 m
~40 m
Spanish Bight
Fault
Multiple
Multiple

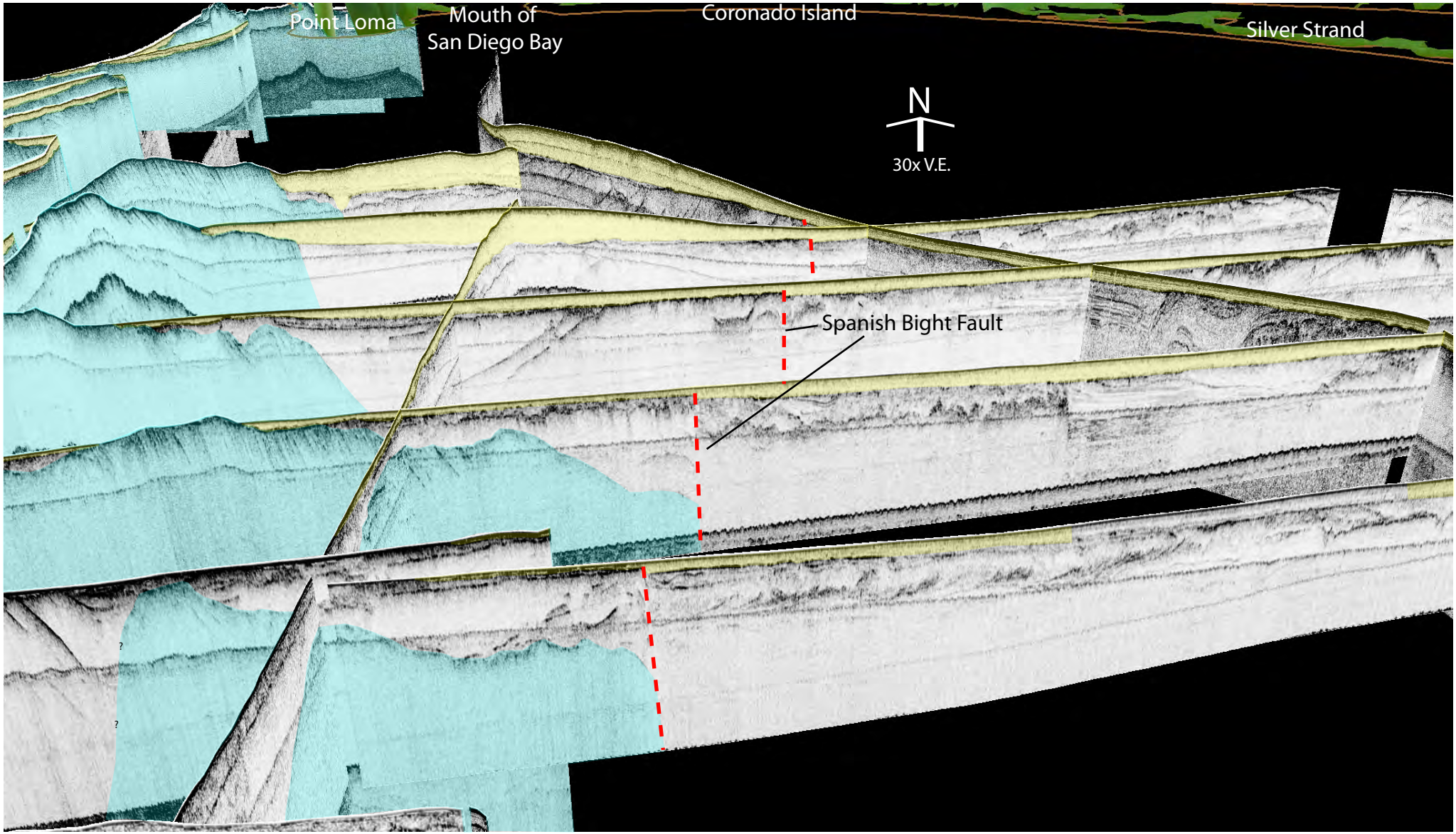
Point Loma
Mouth of
San Diego Bay
Coronado Island
Silver Strand
N
30x V.E.
Spanish Bight Fault

CFZ

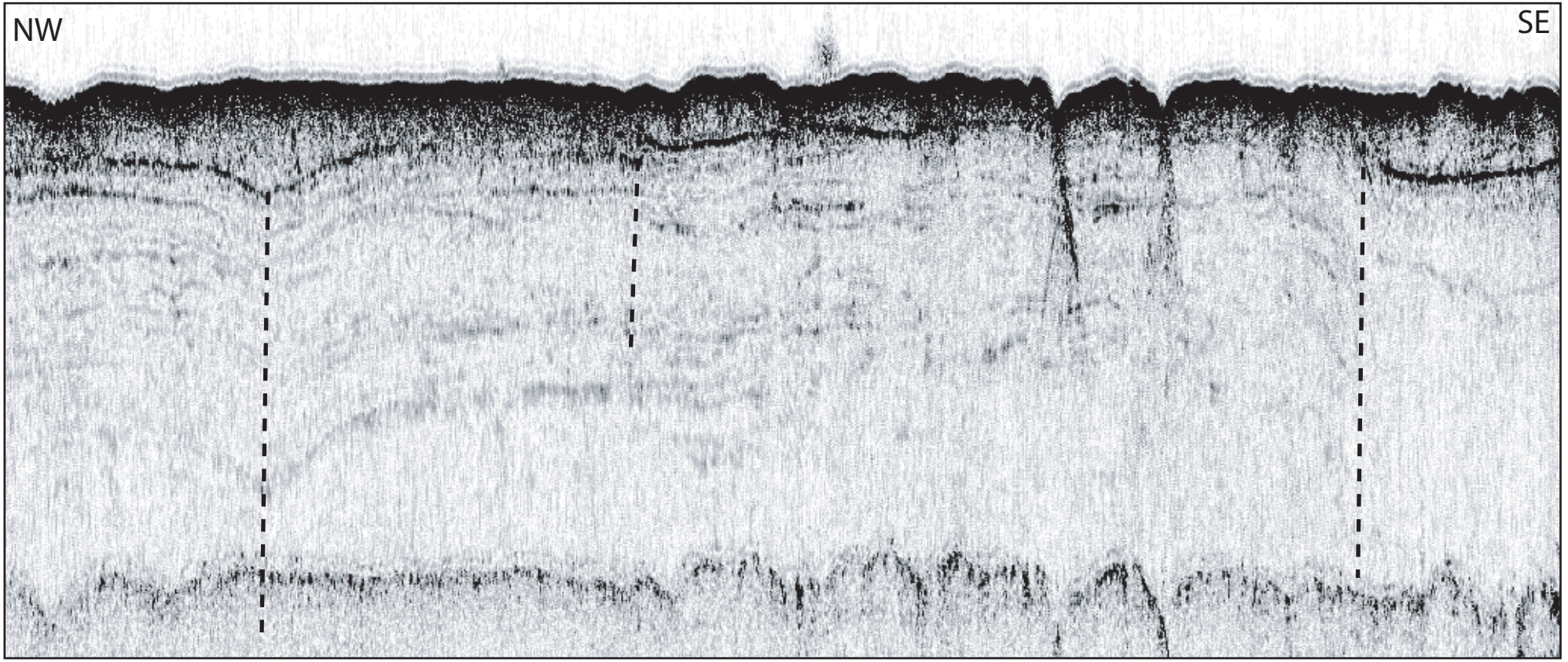

NW SSFZ SE

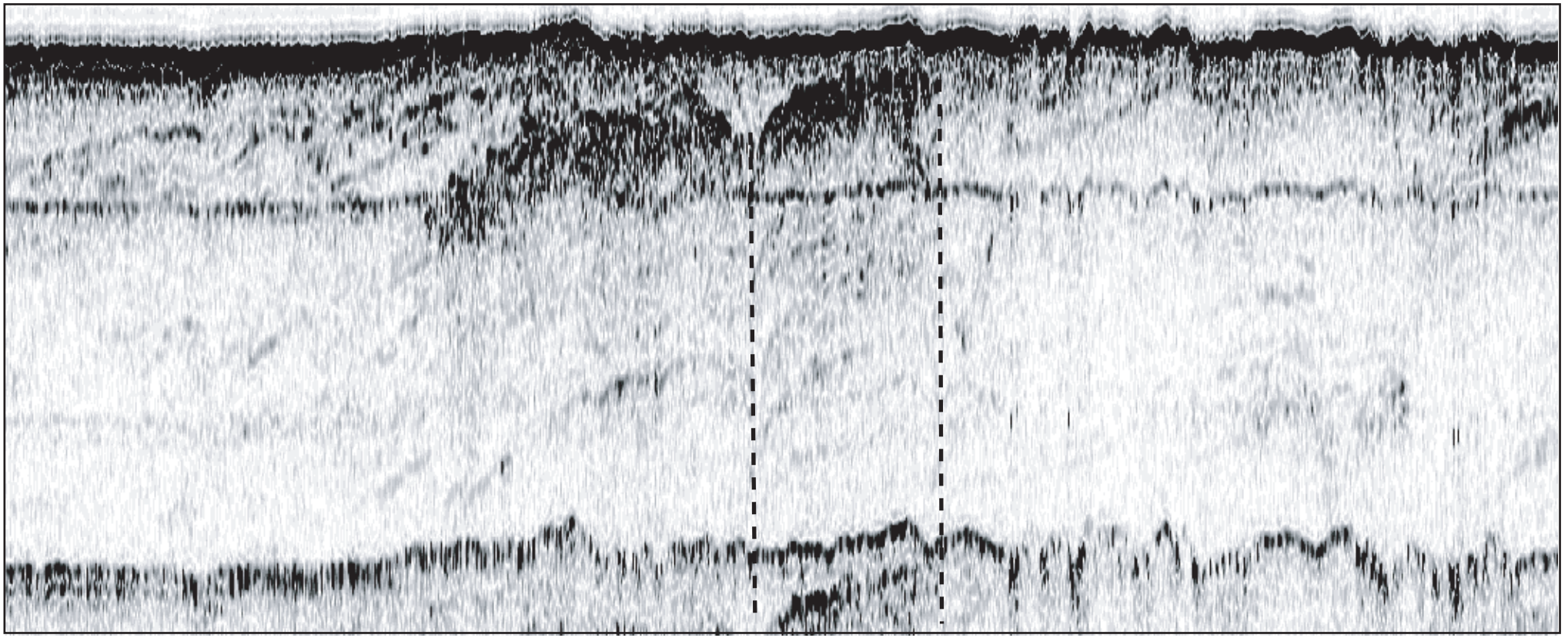

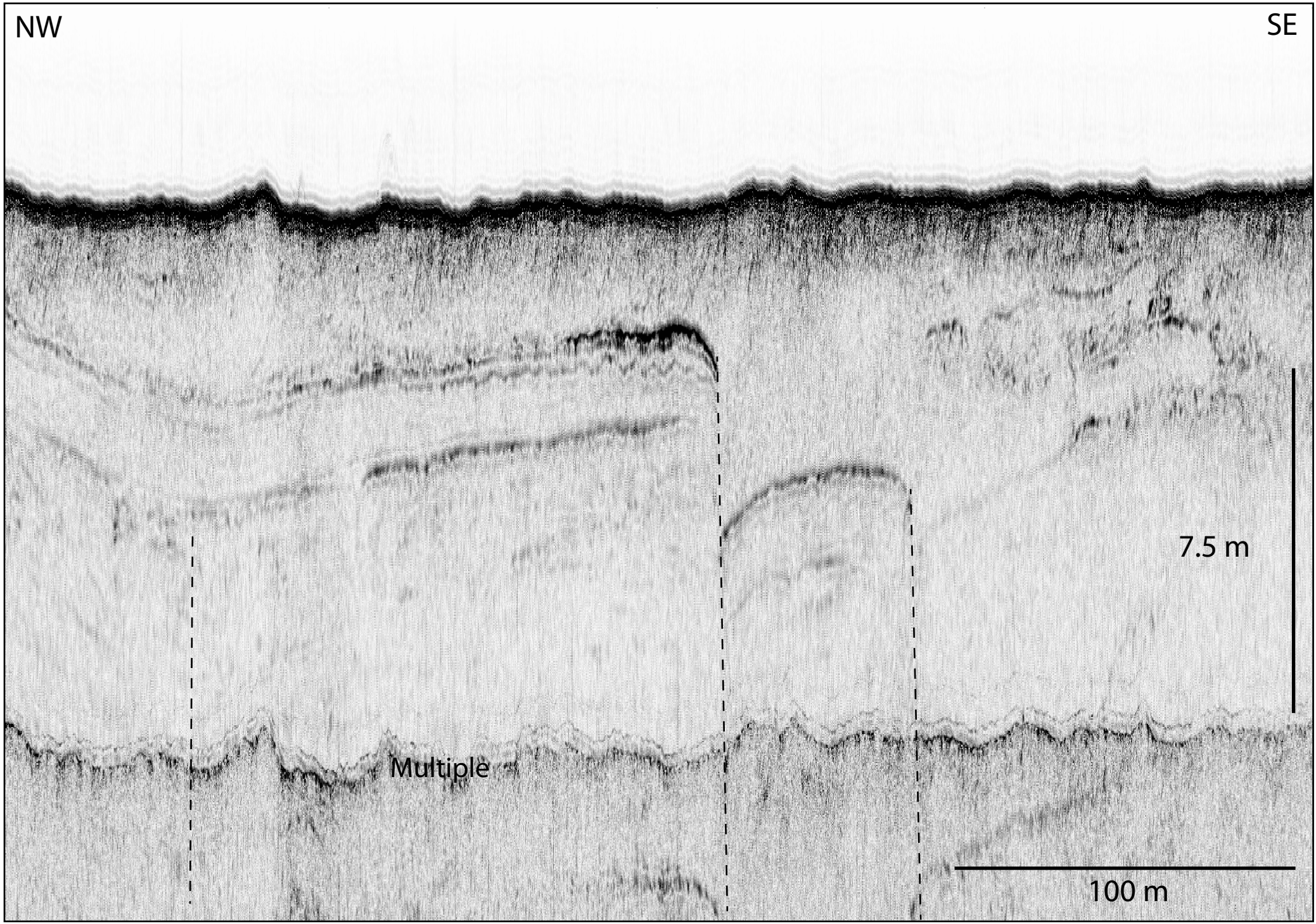
NW
SE
7.5 m
Multiple
100 m